Cardio-Oncology

RESEARCH

Open Access

Machine learning for cardio-oncology: predicting global longitudinal strain from conventional echocardiographic measurements in cancer patients

Tagayasu Anzai[1,2*], Kenji Hirata[2,3,4], Ken Kato[1] and Kohsuke Kudo[2,3,4]

Abstract

Introduction Global longitudinal strain (GLS) is an important prognostic indicator for predicting heart failure and cancer therapy-related cardiac dysfunction (CTRCD). Although access to GLS measurement has increased across institutions, its actual use in clinical practice remains limited due to practical barriers such as limited time and insufficient training. If reduced GLS could be predicted from conventional echocardiographic parameters, it could help identify patients who would most benefit from direct GLS assessment. Therefore, in this study, we tested the hypothesis that reduced GLS can be predicted from conventional echocardiography via a machine learning (ML) approach.

Methods This single-center cross-sectional study included patients who visited the Tokyo Metropolitan Tama Medical Center Hospital and underwent echocardiography with GLS before or after anticancer chemotherapy. Low-GLS was defined as a GLS < 16; otherwise, it was defined as Normal-GLS. Patients with EF < 50% were excluded. We developed ML models that predict Low-GLS from conventional echocardiography measurements. Sixteen ML models were constructed including various boosting and tree-based methods. We assessed the models by the area under the receiver operating characteristic curve (AUC), accuracy, sensitivity, specificity, Positive predictive value (PPV), Negative predictive value (NPV), and F1 score. The Shapley Additive exPlanations (SHAP) method was employed to evaluate the essential predictors.

Results A total of 1,484 patients (64 ± 13 years old, 69% female) were enrolled for ML model development, including 406 patients with Low-GLS and 1,078 with Normal-GLS. The best model for the test dataset was the CatBoost classifier (AUC, 0.748; accuracy, 0.734). Diastolic dysfunction indices [such as septal/lateral mitral annular early diastolic velocity (e') and E-wave to atrial contraction filling velocity (E/A)] and peak velocity-related parameters [aortic valve peak velocity (AV-Vmax) and left ventricular outflow tract velocity maximum (LVOT-Vmax)] played essential roles in the Low-GLS prediction model.

*Correspondence:
Tagayasu Anzai
tagayasu@hawaii.edu

Full list of author information is available at the end of the article

Conclusion This study indicated the possibility that Low-GLS might be predicted by machine learning models from conventional echocardiography measurements in cancer patients.

Keywords Machine learning, Global longitudinal strain, CTRCD

Introduction

Progress in medical care has decreased cancer-related mortality and incidence rates, resulting in an extended average lifespan [1]. Cardiovascular diseases are the most significant factors affecting cancer patients following cancer recurrence [2], often leading to fatal outcomes [3]. Cancer therapy-related cardiac dysfunction (CTRCD) encompasses various types of cardiac impairments induced by cancer treatments, such as chemotherapy, targeted drugs, radiation therapy, and immunotherapy [4].

Global longitudinal strain (GLS) measures myocardial deformation that reflects the shortening of myocardial fibers in the longitudinal direction. It is useful for detecting CTRCD [5].

Observational studies have shown that although absolute measurements of GLS, both at baseline and during therapy, are predictive of CTRCD risk [6]. CTRCD is defined as a relative reduction in GLS from a baseline of 15% or more [7]. A meta-analysis reported that normal values of GLS varied from approximately − 16% to -22% [8], and the lower boundary of GLS with a normal EF was − 16% [8]. GLS-guided cardioprotective therapy has been shown to prevent a reduction in the left ventricular ejection fraction (EF) and the development of CTRCD in high-risk patients undergoing potentially cardiotoxic cancer therapy [9].

Although the availability of equipment and software for measuring GLS has become widespread, the actual implementation of GLS measurement in clinical practice remains limited. For example, an international survey conducted by the European Association of Cardiovascular Imaging (EACVI) reported that while 98% of respondents had access to speckle-tracking echocardiography (STE), only 39% routinely performed and reported STE results in more than 50% of their patients due to practical barriers such as limited time and insufficient training [10]. Given this reality, we believe that incorporating the machine learning approach developed in this study into echocardiographic practice could help identify patients at risk of reduced GLS and prompt clinicians to perform direct GLS measurements when most needed. Therefore, we tested the hypothesis that Low-GLS (GLS < 16%) in cancer patients could be predicted via conventional echocardiography measurements through a machine learning (ML) approach.

Methods

Patient cohort and study design (Fig. 1)

This single-center cross-sectional study included patients who visited the Tokyo Metropolitan Tama Medical Center Hospital between April 1, 2020, and September 30, 2024, and who underwent echocardiography with GLS before or after anticancer chemotherapy ($n = 1{,}531$). Patient characteristics such as age, gender, body mass index (BMI), and conventional echocardiographic measurements were collected. Patients whose left ventricular EF was less than 50% ($n = 47$) were excluded from the analysis. As a result, 1,484 patients were enrolled for ML model development. ML (PyCaret; see *Machine-Learning Framework*) was performed with a 4:1 ratio for random assignment to the training and test datasets. The study protocol adhered to the Declaration of Helsinki and was approved by the Institutional Review Board (IRB) of the Tokyo Metropolitan Tama Medical Center, with an opt-out option for patients (Ethics Approval No.5–37). As this study was retrospective, the requirement for informed consent was waived by the IRB. The corresponding author had full access to all the study data and was also responsible for the data analysis.

Transthoracic echocardiography

The echocardiograms were measured on an Epiq Elite ultrasound machine (Philips Medical Systems, Andover, MA, USA) via an X5-1 matrix transducer. Clinical laboratory technicians performed all echocardiograms; a certificated cardiologist verified all echocardiographic images. To evaluate GLS, we used the Philips QLAB (Version:15.5) cardiac analysis application "AutoStrain" (Phillips Healthcare, Eindhoven, The Netherlands) [11]. Patients whose GLS was smaller than 16% were defined as having Low-GLS, and the others were defined as having Normal-GLS [8]. In addition to GLS, 24 conventional echocardiographic measurements were collected (Table 1).

Machine-learning framework

The PyCaret 3.0 library (https://pycaret.org) is a high-lev el, user-friendly machine-learning framework written in Python in a low-code environment [12]. PyCaret, which also contains Numpy, Pandas, and scikit-learn, streamlines model construction and evaluation [12] by automating data preparation, feature engineering, and model selection activities. We constructed multiple non-deep machine learning models via PyCaret [12].

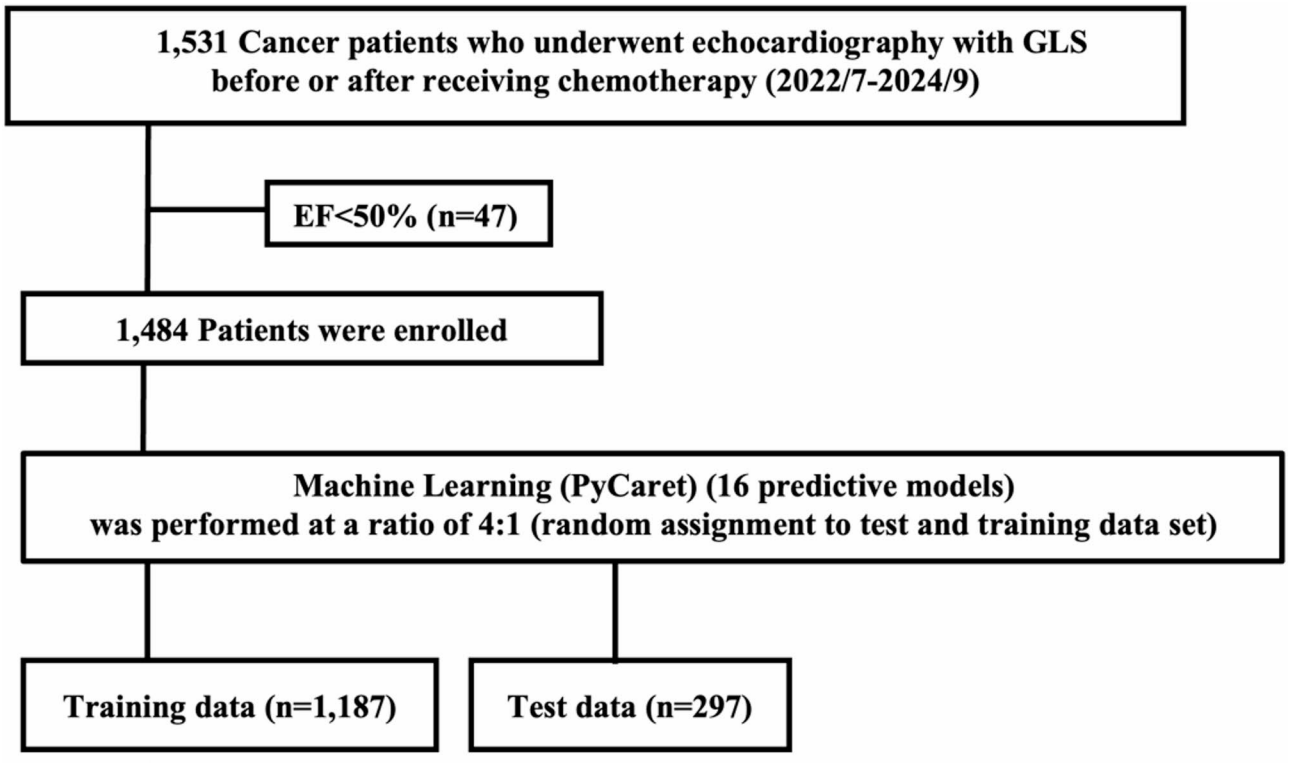

Fig. 1 Study design
GLS, Global Longitudinal Strain; EF, ejection fraction

Table 1 Echocardiographic measurements

No.	Variable Name	Description/Unit
1	Aortic regurgitation (AR)	(Present or absent)*
2	Aortic root diameter (AAD)	(mm)
3	Aortic valve peak velocity (AV-Vmax)	(m/sec)
4	Atrial contraction filling velocity (A)	(m/sec)
5	Deceleration time of the E wave (DCT)	(ms)
6	Ejection fraction (EF)	(%)
7	Global Longitudinal Strain (GLS)	(%)
8	Interventricular septal thickness (IVST)	(mm)
9	Left atrial diameter (LAD)	(mm)
10	Left ventricular diastolic diameter (LVDd)	(mm)
11	Left ventricular systolic diameter (LVDs)	(mm)
12	Left ventricular mass index (LVMI)	(g/m2)
13	Left ventricular outflow maximum diastolic velocity (LVOT-Vmax)	(mm)
14	Left ventricular wall thickness (PWT)	(mm)
15	Mitral regurgitation (MR)	(Present or absent)*
16	Pericardial effusion	(Present or absent)*
17	Pulmonary regurgitation (PR)	(Present or absent)*
18–19	Septal/lateral atrial contraction myocardial velocity (Septal a'/lateral a')	(cm/sec)
20–21	Septal/lateral mitral annulus early diastolic velocity (Septal e'/lateral e')	(cm/sec)
22	Transmitral early diastolic filling velocity to atrial contraction filling velocity (E/A) (Ratio)	
23	Transmitral early diastolic filling velocity to mitral annulus early diastolic velocity (E/e') (Ratio)	
24	Transmitral early filling velocity (E)	(cm/sec)
25	Tricuspid regurgitation (TR)	(Present or absent)

*Regurgitations, including AR, MR, PR, and TR, were defined as present if they were observed with a severity of mild or greater

Exploratory data analysis

Continuous variables were compared via an independent t test or the Mann–Whitney test, depending on the variable distribution tested with the Kolmogorov-Smirnov test. Categorical variables were reported as percentages in numbers and were compared via the chi-square test or Fisher's exact test, if appropriate. We performed all the statistical exploratory data analyses via SAS 9.4 (SAS Institute Inc., Cary, NC, USA). Continuous variables are shown as the mean ± standard deviation (SD).

Setting up the environment and preprocessing in machine learning

For our machine learning analysis, we used the hold-out method. The data were randomly divided into training and test datasets in a 4:1 (n = 1,187 and n = 297) ratio. We performed collinearity analysis, which is commonly used to reduce dimensions as feature selection. The Pearson correlation test was used to analyze collinearity between the variables. The feature selection threshold was 0.60. Data normalization was performed in the analysis using the z-score method to standardize the features.

Training and fine-tuning models

We trained ML models and evaluated their performance on the test dataset using 26 variables (age, gender, and 24 conventional echocardiography measurements: Table 1). Initially, the study compared the performance of 16 ML algorithms (Supplemental Table 2) without hyperparameter optimization using the PyCaret framework through 10-fold cross-validation in the training dataset. We then executed optimization procedures for each ML model. Hyperparameter tuning was conducted using the Optuna method [13]. All the tuned models used the training dataset to construct the final models, whose diagnostic performance was subsequently evaluated on the test dataset. Metrics such as accuracy, sensitivity (recall), specificity, positive predictive value (PPV: precision), negative predictive value (NPV), F1 score, and area under the receiver operating characteristic curve (AUC) were used to assess each model's classification performance on the test dataset. Finally, the top five models were selected based on AUC.

Feature importance and SHAP values

The importance of the model features was evaluated to determine the contribution of each predictor to the ML model. For tree-based models within PyCaret, feature importance was determined based on the reduction in Gini impurity [14]. Additionally, we used Shapley Additive Explanations (SHAP) values to identify and evaluate the most influential features for classifying Low-GLS versus Normal-GLS. SHAP values, derived from cooperative game theory, analyze each feature's contribution to an individual instance's prediction [15]. A feature's SHAP value represents its average marginal contribution to model prediction across all possible feature combinations. The SHAP library computed SHAP values specifically for tree-based models, such as random forests [15].

Results

Characteristics of the participants

A total of 1,484 patients (64 ± 13 y/o, female 69%) were enrolled for ML model development, including 406 patients with Low-GLS and 1,078 with Normal-GLS. The mean age was 67 ± 13 y/o in the Low-GLS group and 63 ± 13 y/o in the Normal-GLS group. Eighteen variables significantly differed between the two groups, including age, gender, and 16 out of 24 (66.7%) echocardiographic measurements (Table 2).

ML prediction model construction and evaluation

Using the 26 variables (age, gender, and 24 conventional echocardiography measurements), the performance of 16 ML algorithms was evaluated. For the training dataset (N = 1,187) using the PyCaret framework's 10-fold cross-validation technique, the ML models achieved AUCs ranging from 0.50 to 0.76 and accuracies ranging from 0.65 to 0.77 without hyperparameter optimization (Supplemental Table 1). We identified the top five ML models with the highest AUC values: CatBoost classifier (CBC), extra trees classifier (ETC), random forest classifier (RFC), gradient boosting classifier (GBC), and logistic regression (LR) (Supplemental Table 1).

All the models were fine-tuned through tenfold cross-validation on training datasets (N = 1,187), and their final performance was assessed on the test datasets (N = 297) (Table 3). Even after fine-tuning, the top-performing machine learning models evaluated by AUC were the CBC, ETC, GBC, RFC, and Quadratic Discriminant Analysis (QDA). The CBC emerged as the best model among these. The CBC achieved an AUC of 0.748 on the test dataset, with an accuracy of 0.734. Figure 2 illustrates the feature importance in CBC. We also assessed the importance of features using the SHAP method (Fig. 3). Diastolic dysfunction indices (septal/lateral e' and E/A) [16] and peak velocity-related parameters (AV-Vmax and LVOT-Vmax) played essential roles in the Low-GLS prediction model.

Feature importance in decision tree models was determined by summing the Gini impurity reductions for each feature across all nodes where the feature was used to split the data. The features were then ranked based on their importance values.

The feature importance for the CatBoost Classifier on the training dataset (a) and test dataset (b), were interpreted using the SHapley Additive exPlanation (SHAP) method. The SHAP is based on "game-theoretic optimal

Table 2 The characteristics of participants

	Total (*n* = 1,484)	Low-GLS (*n* = 406)	Normal-GLS (*n* = 1,078)	*p* value
Age (y/o)	63.7 ± 13.3	66.5 ± 12.8	62.6 ± 13.4	< 0.01
Female, n(%)	69.0%	59.1%	72.7%	< 0.001
BMI (kg/m^2)	22.1 ± 3.8	22.5 ± 4.0	22.0 ± 3.6	< 0.05
EF (%)	66.0 ± 6.0	64.5 ± 6.5	66.6 ± 5.6	< 0.001
GLS(%)	17.7 ± 3.2	13.7 ± 2.0	19.1 ± 2.1	N/A
AAD (mm)	20.5 ± 2.2	21.1 ± 2.4	20.3 ± 2.1	< 0.001
LAD (mm)	31.9 ± 5.5	31.8 ± 6.2	31.9 ± 5.2	0.94
LVDd (mm)	43.0 ± 4.7	42.6 ± 5.2	43.2 ± 4.4	0.02
LVDs (mm)	27.3 ± 3.7	27.5 ± 4.2	27.2 ± 3.5	0.11
IVST (mm)	8.5 ± 1.4	8.8 ± 1.5	8.3 ± 1.4	< 0.001
PWT (mm)	8.5 ± 1.3	8.8 ± 1.4	8.3 ± 1.2	< 0.001
E (cm/s)	70.2 ± 18.2	65.1 ± 17.3	73.5 ± 18.0	< 0.001
A (cm/s)	75.6 ± 20.1	77.8 ± 20.7	74.8 ± 19.8	< 0.05
DCT (ms)	225.5 ± 61.2	228.6 ± 66.4	224.8 ± 59.1	0.28
Septal e` (cm/s)	7.0 ± 2.3	6.1 ± 2.0	7.3 ± 2.3	< 0.001
Septal a` (cm/s)	9.2 ± 1.9	9.0 ± 2.0	9.3 ± 1.8	< 0.01
Lateral e` (cm/s)	9.2 ± 2.8	7.9 ± 2.7	9.5 ± 2.8	< 0.001
Lateral a` (cm/s)	9.9 ± 2.5	9.8 ± 2.4	10.0 ± 2.5	0.12
E/A	1.0 ± 0.4	0.9 ± 0.3	1.0 ± 0.4	< 0.001
E/e'	11.0 ± 4.0	11.5 ± 4.3	10.8 ± 3.8	< 0.01
LVMI (g/m^2)	73.6 ± 18.3	75.4 ± 20.4	72.9 ± 17.5	0.07
AV-Vmax (m/s)	1.4 ± 0.4	1.3 ± 0.4	1.4 ± 0.4	< 0.001
LVOT-Vmax (m/s)	1.0 ± 0.2	0.9 ± 0.2	1.0 ± 0.2	< 0.001
AR, n(%)	15.0%	16.3%	14.5%	0.39
MR, n(%)	29.3%	32.3%	28.2%	0.13
TR, n(%)	36.7%	39.7%	35.5%	0.14
PR, n(%)	7.6%	7.9%	7.5%	0.17
Pericardial effusion, n(%)	14.3%	18.5%	12.7%	< 0.01

Values are presented as numbers, mean ± SD. Continuous variables are analyzed with the t-test or Mann–Whitney U test if data were not normally distributed. Categorical variables are analyzed with the Chi-square test or Fisher's exact test. Significant values are in bold. AAD, Aortic Root Diameter; AR, Aortic Regurgitation (> = mild); AV-Vmax, Aortic Valve Peak Velocity; A, Atrial Contraction Wave; DCT, Deceleration Time of E wave; EF, Ejection Fraction; E/A, Transmitral Early Filling Velocity to Mitral Annular Early Diastolic Velocity Ratio; E, Transmitral Early Filling Velocity; IVST, Interventricular Septal Thickness; LAD, Left Atrium; LVDd, Left Ventricular Diastolic Diameter; LVDs, Left Ventricular Systolic Diameter; LVMI, Left Ventricular Mass Index; LVOT-Vmax, Left Ventricular Outflow Tract Velocity Maximum; MR, Mitral Regurgitation (> = mild); PWT, Left Ventricular Posterior Wall Thickness; TR, Tricuspid Regurgitation (> = mild); e`, Mitral Annular Early Diastolic Velocity; a`, Mitral Annular Atrial Systolic Velocity

Shapley values." In this context, blue indicates patients with Normal-GLS, while red represents those with Low-GLS. The x-axis displays the SHAP value for each feature, where a higher SHAP value (towards the right) signifies a stronger positive contribution to the model's predictions. The three features with the highest absolute SHAP values were LVOT-Vmax, E/A ratio, and PWT.

Discussion

In the present study, we developed and validated machine learning models using PyCaret to predict Low-GLS before and after anticancer chemotherapy. To the best of our knowledge, this is the first study to use ML to predict Low-GLS from conventional echocardiographic measurements in cancer patients. Diastolic dysfunction indices and peak velocity-related parameters played essential roles in the model.

Vendor-specific variations in GLS values

The World Alliance Societies of Echocardiography has proposed normal values for GLS, ranging from 17 to 24% for males and 18–26% for females. GLS is a widely used measurement in echocardiography and applies to other imaging modalities, such as magnetic resonance imaging (MRI) and computed tomography (CT). However, vendor variability has been an issue for GLS. Discrepancies among vendors were first identified in the late 2000s and early 2010s [17, 18]. The European Association of Cardiovascular Imaging (EACVI) and the American Society of Echocardiography (ASE) recognized the importance of standardization and established a task force. In 2010, the EACVI and ASE invited technical representatives from all interested vendors to collaborate in reducing intervendor variability in strain measurements [19, 20]. The task force successfully reduced the differences in GLS between vendors. However, some studies still reported significant intervendor variability, with absolute GLS differences of up to 3.7% between vendors [21]. Because CTRCD diagnosis requires detecting a decrease in GLS of only 15%, even a small reduction in GLS is significant. Therefore, it may be desirable to consistently use the same vendor for patients who require ongoing follow-up. However, in clinical practice, GLS may need to be measured using echocardiography systems from various manufacturers. If a patient needs to have their current GLS measured by echocardiography from a different vendor than before, this study's results might help detect a decrease in GLS.

Although vendor-neutral solutions such as TomTec Imaging Systems GmbH (Munich, Germany), have been developed to minimize intervendor variability, their implementation often remains limited due to cost and operational constraints. Therefore, widespread adoption across all healthcare facilities remains challenging. Alternative approaches that rely on conventional echocardiographic parameters may still offer practical value in settings where vendor-neutral strain analysis solutions are not readily available.

Limitations of GLS measurements

Speckle-tracking software for strain analysis in echocardiography is widely available commercially. Although standardized guidelines for accurately measuring GLS have also recently become more widely accessible, it is sometimes not possible to obtain suitable images for GLS measurement, particularly in cases such as

Table 3 Results of machine learning Low-GLS predictive models by PyCaret

	AUC	ACC	Sensitivity (Recall)	Specificity	PPV (Precision)	NPV	F-1
Training dataset (after fine-tuning)							
CatBoost Classifier	0.7547	0.7709	0.2986	0.9490	0.6794	0.7826	0.4106
Extra Trees Classifier	0.7542	0.7591	0.2187	0.9629	0.6907	0.7658	0.3306
Gradient Boosting Classifier	0.7493	0.7616	0.1788	0.9814	0.7567	0.7604	0.2854
Random Forest Classifier	0.7485	0.7625	0.4309	0.8875	0.5941	0.8058	0.4961
Quadratic Discriminant Analysis	0.7449	0.7439	0.4155	0.8678	0.5447	0.7983	0.4661
Test dataset							
CatBoost Classifier	0.7481	0.7340	0.2469	0.9167	0.7645	0.5263	0.3361
Extra Trees Classifier	0.7217	0.7508	0.1605	0.9722	0.7554	0.6842	0.2600
Gradient Boosting Classifier	0.7572	0.7374	0.1358	0.9630	0.7482	0.5789	0.2200
Random Forest Classifier	0.7321	0.7306	0.3704	0.8657	0.7857	0.5085	0.4286
Quadratic Discriminant Analysis	0.7072	0.7273	0.4074	0.8472	0.7922	0.5000	0.4490

The upper table presents the top five models, ranked by the area under the receiver operating characteristic curve (AUC) for screening performance on the training dataset following fine-tuning. The lower table illustrates the diagnostic performance of these fine-tuned models on the test dataset. ACC, accuracy; NPV, Negative predictive value; PPV, Positive predictive value

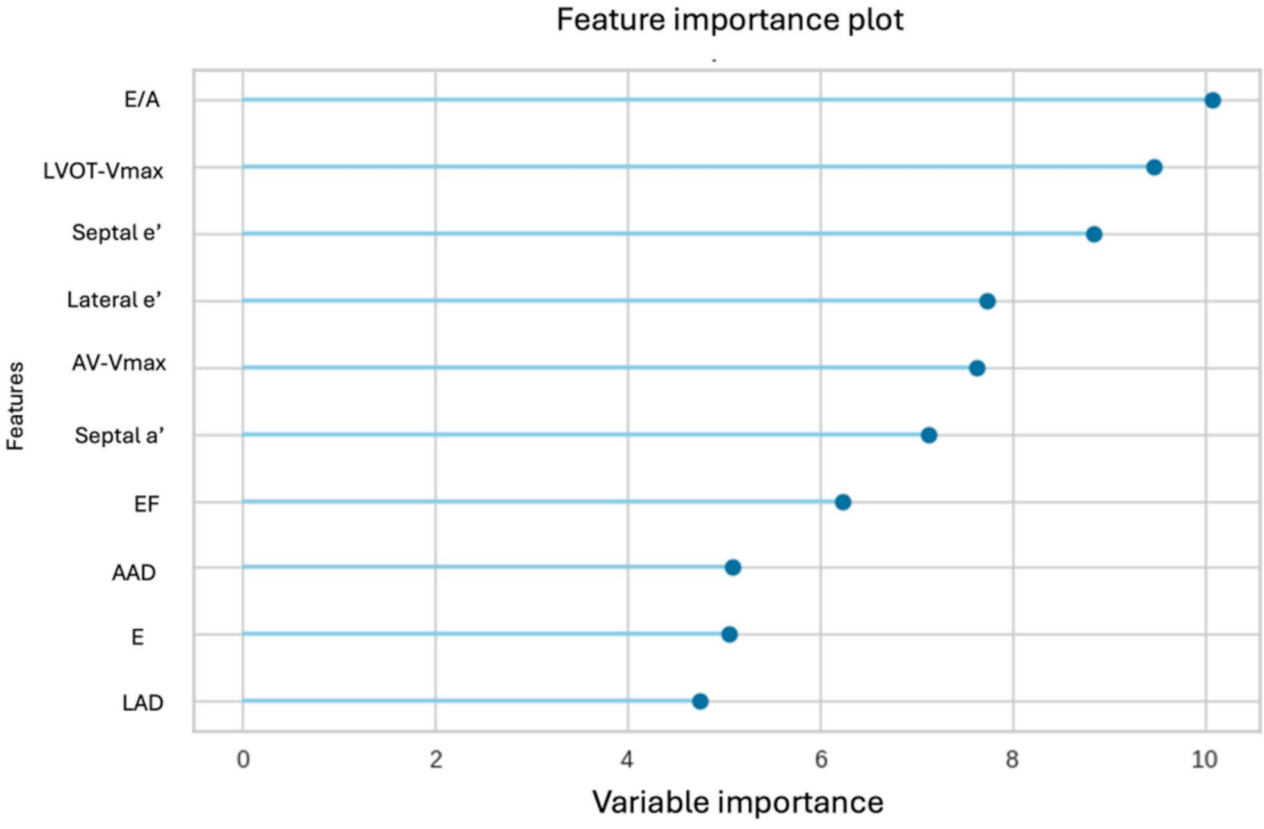

Fig. 2 Feature importance of CatBoost classifier on the training dataset
AAD, Aortic Root Diameter; AV-Vmax, Aortic Valve Peak Velocity; EF, Ejection Fraction; E/A, Transmitral Early Filling Velocity to Mitral Annular Early Diastolic Velocity Ratio; E, Transmitral Early Filling Velocity; LAD, Left Atrium; LVOT-Vmax, Left Ventricular Outflow Tract Velocity Maximum; e', Mitral Annular Early Diastolic Velocity; a, Mitral Annular Atrial Systolic Velocity

post-mastectomy breast cancer patients or those with high BMIs. A reduction in GLS has been observed before a decline in EF with good-quality images, but poor image quality hinders the detection of decreased GLS and reduced reproducibility [22]. Even when suitable GLS images are unavailable, GLS may be predicted using conventional echocardiographic parameters.

Recent advances in AI-based GLS measurement, such as those demonstrated by Patel et al. [23], have shown the potential to improve reproducibility and reduce

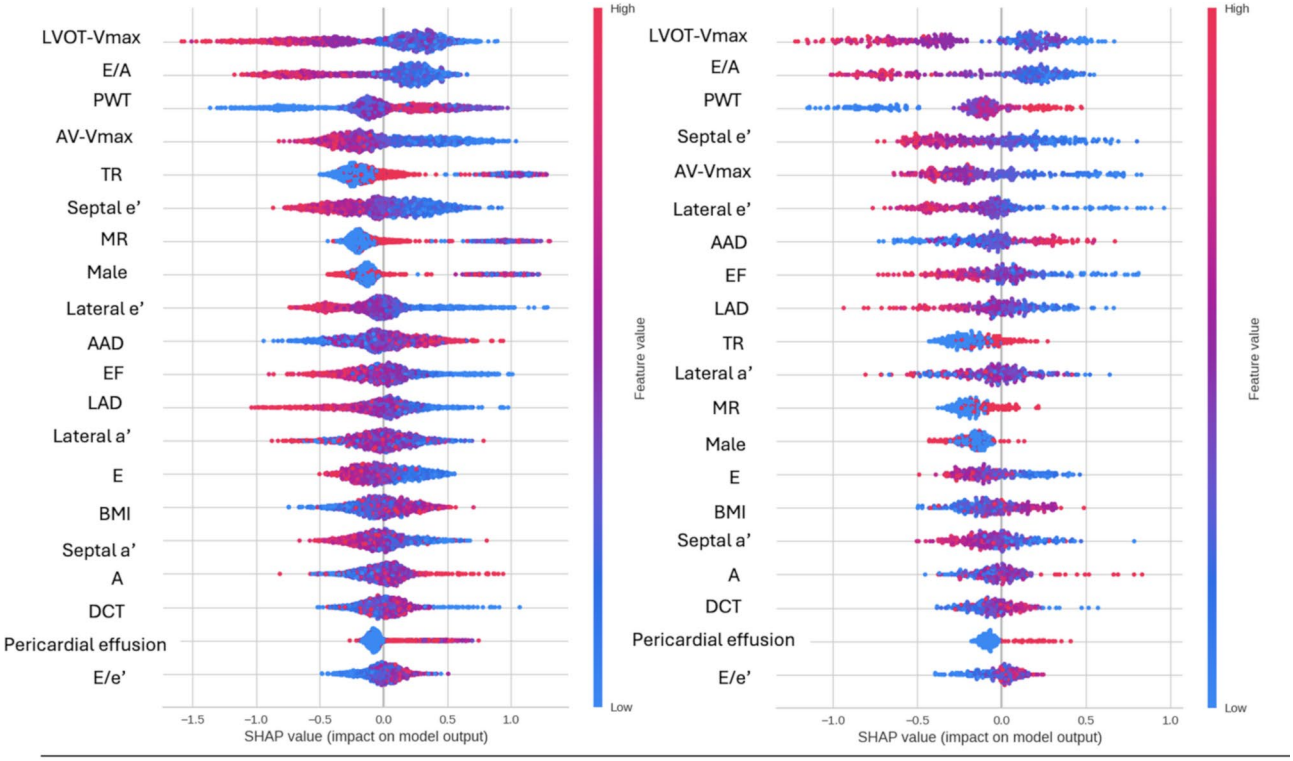

Fig. 3 SHAP method on CatBoost classifier
(**a**) Training dataset. (**b**) Test dataset
AAD, Aortic Root Diameter; AR, Aortic Regurgitation (>=mild); AV-Vmax, Aortic Valve Peak Velocity; A, Atrial Contraction Wave; DCT, Deceleration Time of E wave; EF, Ejection Fraction; E/A, Transmitral Early Filling Velocity to Mitral Annular Early Diastolic Velocity Ratio; E, Transmitral Early Filling Velocity; IVST, Interventricular Septal Thickness; LAD, Left Atrium; W.p.4, Left Ventricular Diastolic Diameter; LVDs, Left Ventricular Systolic Diameter; LVMI, Left Ventricular Mass Index; LVOT-Vmax, Left Ventricular Outflow Tract Velocity Maximum; MR, Mitral Regurgitation (>=mild); PWT, Left Ventricular Posterior Wall Thickness; TR, Tricuspid Regurgitation (>=mild); e', Mitral Annular Early Diastolic Velocity; a', Mitral Annular Atrial Systolic Velocity

observer- and vendor-related variability. In the future, the application of AI-based GLS measurement may enable more accurate assessment of GLS even in cases with poor image quality. Furthermore, combining direct AI-based GLS measurement with AI models that predict GLS impairment from conventional echocardiographic parameters, such as the approach proposed in our study, may further enhance overall diagnostic accuracy. Integrating these complementary methods could contribute to improving the reliability and clinical utility of GLS evaluation across a wider range of patient populations.

CTRCD and left ventricular diastolic dysfunction (LVDD)

Left ventricular diastolic dysfunction (LVDD) affects left ventricular filling and stroke volume. Several studies have shown that LVDD is associated with all-cause mortality in patients with heart failure [24, 25], as well as with CRTCD [26, 27]. In this study, the key factors predicting Low-GLS, such as septal/lateral e‘ and E/A, were also indicators of LVDD [16]. The findings of this study may suggest that in cases where EF is preserved, but GLS is reduced after chemotherapy, diastolic dysfunction may also be present. The assessment of diastolic parameters via echocardiography might also be recommended in populations treated with chemotherapy alongside the GLS assessment.

Strengths and limitations

This is the first study to employ ML to predict reduced GLS based on conventional echocardiographic measurements in cancer patients. Several limitations of this study should be considered. First, this was a single-center study, and external validation has not yet been performed. Although we demonstrated moderate diagnostic performance, the lack of validation in independent populations significantly limits the broader applicability and generalizability of our findings. Without external validation across diverse institutions and patient populations, the robustness and reproducibility of the model cannot be fully confirmed. To ensure generalizability and potential clinical utility, external validation through multicenter, prospective cohorts will be essential. Second, due to the cross-sectional nature of the study design, this ML model cannot predict changes in GLS following anticancer drug administration or patient prognosis. This limitation restricts the model's ability to support longitudinal

patient monitoring, which is one of the key benefits of GLS analysis during oncological therapy. In future studies, we plan to collect longitudinal echocardiographic data and develop models capable of predicting temporal changes in GLS, thereby enhancing the clinical utility of ML-based approaches. Third, the variables used in this study did not include myocardial contractility indicators that could serve as alternatives to GLS, such as MAPSE (mitral annular plane systolic excursion), which assesses the longitudinal movement of the mitral annulus during systole, and s' (systolic velocity of the mitral annulus), which is measured by tissue Doppler imaging. The Incorporation of these indices will facilitate the development of more accurate models. However, as of 2025, since MAPSE and s' are not routinely measured in clinical practice, GLS measurement should be a viable option in facilities capable of assessing MAPSE and s'. In the future, we would like to consider developing models that incorporate MAPSE and s' measurements, as these indices may offer additional value, particularly in cases where GLS assessment is limited by suboptimal image quality.

Fourth, the use of a dichotomous classification of GLS in this study limits its direct applicability to clinical practice. Although the binary approach served as a practical first step given the available sample size and model performance, future efforts should focus on developing more granular models, such as categorizing GLS into three groups (e.g., GLS > 20%, GLS 16–20%, and GLS < 16%) or predicting GLS as a continuous variable to better support clinical decision-making.

Fifth, although we demonstrated an AUC of 0.75, this level of performance is not sufficient for definitive clinical decision-making. However, in certain contexts—such as initial screening or prioritization in resource-limited settings—this level of discrimination may still be practically useful. Importantly, in our threshold analysis, when sensitivity was increased to 80% to minimize missed cases of reduced GLS, specificity declined to approximately 40%. Conversely, improving specificity to 80% reduced sensitivity to around 50%. These findings highlight the trade-off between sensitivity and specificity. Despite these limitations, the model may still serve as a valuable tool for early risk identification and guiding selective GLS measurement, especially where routine strain imaging is not feasible. Future research should focus on enhancing model accuracy and sensitivity by incorporating larger and more diverse datasets.

Sixth, in this study, cases with poor image quality were naturally excluded, as we only included examinations where GLS measurement was successfully performed. Consequently, there is a selection bias toward patients with relatively good image quality. Given that the model was trained on these biased data, it is likely that the predictive performance of the model, based on the 24 echocardiographic parameters, would decline when applied to cases with suboptimal image quality. In the future, to develop models that are more robust to variations in image quality, additional strategies may be necessary, such as incorporating GLS measurements obtained through cardiac MRI in cases where echocardiographic GLS assessment is not feasible.

Seventh, some conventional echocardiographic parameters used in this study are subject to angle dependence, unlike GLS, which is angle-independent. As a result, suboptimal imaging angles may reduce the predictive accuracy of the model. Future studies should assess model performance under conditions of suboptimal image acquisition.

Conclusions

This study suggests that Low-GLS can be predicted using conventional echocardiography with an ML approach, which may be helpful in remote areas without GLS measurement or in cases where echocardiography machines from the same manufacturer cannot be used.

Abbreviations

A	Atrial contraction filling velocity
AAD	Aortic root diameter
AUC	Area-under-the-curve
AR	Aortic regurgitation
ASE	American Society of Echocardiography
AV-Vmax	Aortic valve peak velocity
BMI	Body mass index
CBC	CatBoost classifier
CTRCD	Cancer therapy-related cardiac dysfunction
DCT	Deceleration time of the E wave
E	Transmitral early filling velocity
E/A	Transmitral early diastolic filling velocity to atrial contraction filling velocity
E/e'	Transmitral early diastolic filling velocity to mitral annulus early diastolic velocity
EACVI	European Association of Cardiovascular Imaging
EF	Ejection fraction
ETC	Extra trees classifier
GBC	Gradient boosting classifier
GLS	Global Longitudinal Strain
IVST	Interventricular septal thickness
LAD	Left atrial diameter
Lateral a'	Lateral atrial contraction myocardial velocity
Lateral e'	Lateral mitral annulus early diastolic velocity
LR	Logistic regression
LVDd	Left ventricular diastolic diameter
LVDD	Left ventricular diastolic dysfunction
LVDs	Left ventricular systolic diameter
LVMI	Left ventricular mass index
LVOT-Vmax	Left ventricular outflow maximum diastolic velocity
MAPSE	Mitral annular plane systolic excursion
ML	Machine learning
MR	Mitral regurgitation
NPV	Negative predictive value
PPV	Positive predictive value
PR	Pulmonary regurgitation
PWT	Left ventricular wall thickness
QDA	Quadratic Discriminant Analysis
RFC	Random forest classifier
s'	Systolic velocity of the mitral annulus
Septal a'	Septal atrial contraction myocardial velocity
Septal e'	Septal mitral annulus early diastolic velocity

SHAP	Shapley Additive exPlanations
STE	Speckle-Tracking Echocardiography
TR	Tricuspid regurgitation

Supplementary Information

The online version contains supplementary material available at https://doi.org/10.1186/s40959-025-00348-z.

Supplementary Material 1

Acknowledgements
N/A.

Author contributions
Conceptualization, T.Anzai. and K.Hirata.; Methodology, T.Anzai. and K.Hirata; Experiment and Validation, T.Anzai.; Writing-Original Draft Preparation, T.Anzai. and K.Hirata.; Writing-Review & Editing, K.Kato. and K.Kudo.
All authors have read and agreed to the published version of the manuscript.

Funding
This research received no funding.

Data availability
The datasets used and/or analyzed during the current study are available from the corresponding author on reasonable request.

Declarations

Ethics approval and consent to participate
The study protocol adhered to the Declaration of Helsinki and was approved by the Institutional Review Board (IRB) of the Tokyo Metropolitan Tama Medical Center, with an opt-out option for patients (Ethics Approval No.5–37). As this study was retrospective, the requirement for informed consent was waived by the IRB.

Competing interests
The authors declare that there are no conflicts of interests regarding the publication of this paper.

Consent to participate
Not applicable.

Author details
[1]Cardiology Department, Tokyo Metropolitan Tama Medical Center, Fuchu, Japan
[2]Clinical AI Human Resources Development Program (CLAP), Faculty of Medicine, Hokkaido University, Sapporo, Japan
[3]Department of Diagnostic and Interventional Radiology, Faculty of Medicine, Hokkaido University, Sapporo, Japan
[4]Medical AI Research and Development Center, Hokkaido University Hospital, Sapporo, Japan

Received: 15 February 2025 / Accepted: 6 May 2025
Published online: 22 May 2025

References

1. Dent SF, Kikuchi R, Kondapalli L, Ismail-Khan R, Brezden-Masley C, Barac A, Fradley M. Optimizing cardiovascular health in patients with cancer: A practical review of risk assessment, monitoring, and prevention of Cancer Treatment–Related cardiovascular toxicity. Am Soc Clin Oncol Educational Book. 2020;40:501–15.
2. Yoon DW, Shin DW, Cho JH, Yang JH, Jeong S-M, Han K, Park SH. Increased risk of coronary heart disease and stroke in lung cancer survivors: A Korean nationwide study of 20,458 patients. Lung Cancer. 2019;136:115–21.
3. Liu D, Ma Z, Yang J, Zhao M, Ao H, Zheng X, Wen Q, Yang Y, You J, Qiao S et al. Prevalence and prognosis significance of cardiovascular disease in cancer patients: a population-based study. (1945–4589 (Electronic)).
4. Lyon AR, López-Fernández T, Couch LS, Asteggiano R, Aznar MC, Bergler-Klein J, Boriani G, Cardinale D, Cordoba R, Cosyns B, et al.: 2022 ESC guidelines on cardio-oncology developed in collaboration with the European hematology association (EHA), the European society for therapeutic radiology and oncology (ESTRO) and the international Cardio-Oncology society (IC-OS): developed by the task force on cardio-oncology of the European society of cardiology (ESC). Eur Heart J. 2022;43(41):4229–361.
5. Calvillo-Argüelles O, Thampinathan B, Somerset E, Shalmon T, Amir E, Steve Fan C-P, Moon S, Abdel-Qadir H, Thevakumaran Y, Day J, et al. Diagnostic and prognostic value of myocardial work indices for identification of Cancer Therapy–Related cardiotoxicity. JACC: Cardiovasc Imaging. 2022;15(8):1361–76.
6. Marwick TA-O. Global Longitudinal Strain Monitoring to Guide Cardioprotective Medications During Anthracycline Treatment. (1534–6269 (Electronic)).
7. Chang H-Y, Lee C-H, Su P-L, Li S-S, Chen M-Y, Chen Y-P, Hsu Y-T, Tsai W-C, Liu P-Y, Chen T-Y, et al. Subtle cardiac dysfunction in lymphoma patients receiving low to moderate dose chemotherapy. Sci Rep. 2021;11(1):7100.
8. Potter E, Marwick TH. Assessment of Left Ventricular Function by Echocardiography: The Case for Routinely Adding Global Longitudinal Strain to Ejection Fraction. *JACC: Cardiovascular Imaging* 2018, 11(2, Part 1):260–274.
9. Thavendiranathan P, Negishi T, Somerset E, Negishi K, Penicka M, Lemieux J, Aakhus S, Miyazaki S, Shirazi M, Galderisi M, et al. Strain-Guided management of potentially cardiotoxic Cancer therapy. J Am Coll Cardiol. 2021;77(4):392–401.
10. Sade LE, Joshi SS, Cameli M, Cosyns B, Delgado V, Donal E, Edvardsen T, Carvalho RF, Manka R, Podlesnikar T, et al. Current clinical use of speckle-tracking strain imaging: insights from a worldwide survey from the European association of cardiovascular imaging (EACVI). Eur Heart J Cardiovasc Imaging. 2023;24(12):1583–92.
11. Kawakami H, Wright L, Nolan M, Potter EL, Yang H, Marwick TH. Feasibility, reproducibility, and clinical implications of the novel fully automated assessment for global longitudinal strain. J Am Soc Echocardiogr. 2021;34(2):136–e145132.
12. Gain U, Hotti V. Low-code AutoML-augmented Data Pipeline– A Review and Experiments. *Journal of Physics: Conference Series* 2021, 1828(1).
13. Akiba T, Sano S, Yanase T, Ohta T, Koyama M. Optuna: A Next-generation Hyperparameter Optimization Framework; 2019.
14. Gogishvili D, Vromen EM, Koppes-den Hertog S, Lemstra AW, Pijnenburg YAL, Visser PJ, Tijms BM, Del Campo M, Abeln S, Teunissen CE, et al. Discovery of novel CSF biomarkers to predict progression in dementia using machine learning. Sci Rep. 2023;13(1):6531.
15. Lundberg SM, Erion G, Chen H, DeGrave A, Prutkin JM, Nair B, Katz R, Himmelfarb J, Bansal N, Lee S-I. From local explanations to global Understanding with explainable AI for trees. Nat Mach Intell. 2020;2(1):56–67.
16. Nagueh SF, Smiseth OA, Appleton CP, Byrd BF 3rd, Dokainish H, Edvardsen T, Flachskampf FA, Gillebert TC, Klein AL, Lancellotti P, et al. Recommendations for the evaluation of left ventricular diastolic function by echocardiography: an update from the American society of echocardiography and the European association of cardiovascular imaging. J Am Soc Echocardiogr. 2016;29(4):277–314.
17. Marwick TH. Consistency of myocardial deformation imaging between vendors. Eur J Echocardiogr. 2010;11(5):414–6.
18. Bansal M, Cho G-Y, Chan J, Leano R, Haluska BA, Marwick TH. Feasibility and accuracy of different techniques of Two-Dimensional speckle based strain and validation with harmonic phase magnetic resonance imaging. J Am Soc Echocardiogr. 2008;21(12):1318–25.
19. Voigt JU, Pedrizzetti G, Lysyansky P, Marwick TH, Houle H, Baumann R, Pedri S, Ito Y, Abe Y, Metz S, et al. Definitions for a common standard for 2D speckle tracking echocardiography: consensus document of the EACVI/ASE/Industry task force to standardize deformation imaging. J Am Soc Echocardiogr. 2015;28(2):183–93.
20. Thomas JD, Badano LP. EACVI-ASE-industry initiative to standardize deformation imaging: a brief update from the co-chairs. Eur Heart J Cardiovasc Imaging. 2013;14(11):1039–40.
21. Farsalinos KE, Daraban AM, Ünlü S, Thomas JD, Badano LP, Voigt J-U. Head-to-Head comparison of global longitudinal strain measurements among nine different vendors: the EACVI/ASE Inter-Vendor comparison study. J Am Soc Echocardiogr. 2015;28(10):1171–e11811172.
22. Iida N, Tajiri K, Ishizu T, Sasamura-Koshizuka R, Nakajima H, Kawamatsu N, Sato K, Yamamoto M, Machino-Ohtsuka T, Bando H, et al. Echocardiography image quality of global longitudinal strain in cardio-oncology: a prospective real-world investigation. J Echocardiogr. 2022;20(3):159–65.

23. Patel R, Hussain K, Sanagala T, Robin J, Karagodin I. Fully automated machine learning based echocardiographic assessment of global longitudinal strain in breast Cancer patients receiving cardiotoxic chemotherapy. Circulation. 2024;150(Suppl1):A4144553–4144553.
24. Bursi F, Weston SA, Redfield MM, Jacobsen SJ, Pakhomov S, Nkomo VT, Meverden RA, Roger VL. Systolic and diastolic heart failure in the community. JAMA. 2006;296(18):2209–16.
25. Owan TE, Hodge Do Fau - Herges RM, Herges Rm Fau - Jacobsen SJ, Jacobsen Sj Fau - Roger VL, Roger Vl Fau -, Redfield MM, Redfield MM. Trends in prevalence and outcome of heart failure with preserved ejection fraction. *N Engl J Med* 2006, 355:251–259.
26. Minotti G, Reggiardo G, Camilli M, Salvatorelli E, Menna P. From cardiac anthracycline accumulation to Real-Life risk for early diastolic dysfunction: A translational approach. JACC CardioOncol. 2022;4(1):139–40.
27. Calabrese V, Menna P, Annibali O, Armento G, Carpino A, Cerchiara E, Greco C, Marchesi F, Spallarossa P, Toglia G, et al. Early diastolic dysfunction after Cancer chemotherapy: primary endpoint results of a multicenter Cardio-Oncology study. Chemotherapy. 2018;63(2):55–63.

Publisher's note